Nano Structures of Group 13–15 Mixed Heptamer Clusters: A Computational Study

ARTICLE *in* THE JOURNAL OF PHYSICAL CHEMISTRY A · APRIL 2012

Impact Factor: 2.69 · DOI: 10.1021/jp302323x · Source: PubMed

2 AUTHORS:

Afshan Mohajeri
Shiraz University
68 PUBLICATIONS **557** CITATIONS
SEE PROFILE

Mahsa Ebadi
Uppsala University
2 PUBLICATIONS **3** CITATIONS
SEE PROFILE

THE JOURNAL OF PHYSICAL CHEMISTRY A

Article

pubs.acs.org/JPCA

Nano Structures of Group 13−15 Mixed Heptamer Clusters: A Computational Study

Afshan Mohajeri* and Mahsa Ebadi

Department of Chemistry, College of Sciences, Shiraz University, Shiraz 71454, Iran

Supporting Information

ABSTRACT: The structural and thermodynamic characteristics of lowest-energy structures of group 13−15 mixed heptamers in two distinct series $[(HM)_k(HM')_l(NH)_7]$ (M, M′ = B, Al, Ga and $k + l = 7$) and $[(HGa)_7(YH)_m(Y'H)_n]$ (Y,Y′ = N, P, As and $m + n = 7$) have been systematically investigated using the density functional approach. Our main goal is to get knowledge of the preferential bonding patterns of the first three rows of group 13−15 elements for the construction of mixed heptameric clusters. Structural parameters, thermodynamic properties of oligomerization reaction, band gaps, and dipole moments of the 18 lowest-energy structures of the studied heptamers in each series are compared to their corresponding binary parents, that is, $[(HM)_7(NH)_7]$ and $[(HGa)_7(YH)_7]$. The stability of different isomer structures is discussed to reveal the competitiveness of group 13 and 15 bonding. Mixed heptamers are predicted to be thermodynamically more stable compared to a mixture of monomers. However, the favorability for the generation of mixed heptamers strongly depends on the nature of inserted metal and nonmetal pairs of group 13−15. Moreover, it is found that among all studied heptamers the smaller band gaps correspond to arsenic containing species which are close to the semiconducting regime, around 4.62−4.98 eV.

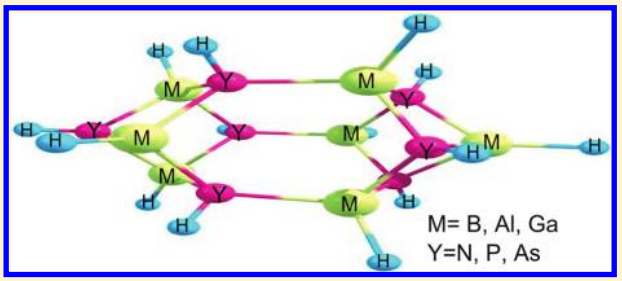

1. INTRODUCTION

Semiconductor nanoparticles promise to play a major role in several new technologies. The intense interest in this area derives from their unique chemical and electronic properties, which gives rise to their potential use in the fields of nonlinear optics, luminescence, electronics, catalysis, solar energy conversion, and optoelectronics, as well as other areas.[1] Chemistry of group 13−15 compounds[2] has grown dramatically in the last 15 years, mostly because of their importance as precursors for 13−15 semiconductors[3−5] as well as intermediates in hydrogen storage technology.[6−9]

From the experimental point of view, the most common way for the production of group 13−15 materials is the chemical vapor deposition (CVD) technique.[10,11] Early synthetic efforts were devoted to develop the technology of deposition of smooth group 13−15 films. In recent years, nanostructured group 13−15 materials have become an extremely hot topic. Instead of manufacturing smooth films and coatings, the experimentalists now turn their attention into fabrication of one, two, and three-dimensional group 13−15 architectures.[12] It was assumed in most of the early studies of the CVD of $A^{III}B^{V}$ compounds that deposition occurred exclusively by the radical or dissociative mechanism. Stable monomeric imides of gallium and aluminum have been synthesized and characterized by Power's group.[13,14] More recent experimental data, however, favor the occurrence of association and the formation of nanoparticles directly in the gas phase during the deposition of GaAs, AlN, and GaN.[15] Formations of the group 13−15 gas-phase stable oligomers may be a good starting point for nanoparticle generation.[16]

Since experimental studies of the gas phase intermediates at high temperatures are very demanding, theoretical approaches become a viable alternative for acquiring the necessary understanding. However, theoretical study of group 13−15 binary compounds $[RMYR']_n$ (M = group 13, Y = group 15 element) is a long-standing area of scientific interest.[17−27] In a comprehensive review in 2008, Timoshkin et al.[28] summarized the results of recent theoretical studies of gas phase reactions leading to nanosized group 13−15 materials.

Apart from binary oligomers of group 13−15, mixed compounds in which the physical properties are controlled by the elemental composition are extremely useful in nanotechnology and microelectronics. For example, the $Al_xGa_y In_{1-x-y}N_z P_{1-z}$ alloy is used as a light emitting diode which emits in the blue, green, yellow, and red spectral regions depending on the composition (x, y, and z).[10,29] However, the production of a composite material with particular desired properties requires exact control of the stoichiometry. Theoretical studies of mixed metal rings were pioneered by Ni and co-workers.[30] Mixed dimeric cyclic compounds $[R_2GaYY'R'_2]_2$ with Ga_2PAs, Ga_2PSb, and Ga_2AsSb cores have been used as precursors toward nanocrystalline gallium-poor GaP_xAs_{1-x}, GaP_xSb_{1-x}, and $GaAs_xSb_{1-x}$.[31,32] The structure and stability of the trimeric $[BAlGaNPAs]H_6$ containing all different group 13 and group 15 elements in the ring and their dimers $[BAlGaNPAs]_2 H_{12}$ have

Received: March 10, 2012
Revised: April 16, 2012
Published: April 16, 2012

been theoretically investigated by Timoshkin and Frenking.[33] Moreover, mixed cubic clusters $[(HAl)_x(HGa)_y(HIn)_z(YH)_4]$ (Y = N, P, As, $x + y + z = 4$) and $[(HM)_4(NH)_k(PH)_l(AsH)_m]$ (M = Al, Ga, In, $k + l + m = 4$) have been theoretically studied.[34]

As far as we know no heptamer cluster containing two different elements of group 13 or group15 have been investigated theoretically or experimentally. Accordingly, in the present work we study group 13−15 ternary composites of the needle-shaped heptamers. Our main goal is to obtain knowledge of the preferential bonding patterns of the first three rows of group 13−15 elements for the construction of mixed heptameric clusters. To address this problem, systematic calculations have been performed on the series of compounds with formal composition of $[(HM)_k(HM')_l[(NH)_7]$ (M, M′ = B, Al, Ga and $k + l = 7$) and $[(HGa)_7(YH)_m(Y'H)_n]$ (Y,Y′ = N, P, As and $m + n = 7$). For the sake of comparison, the structure, stability, and thermodynamic characteristics of the resultant compounds have been compared to the binary clusters of $[(HM)_7(NH)_7]$ and $[(HGa)_7(YH)_7]$.

2. COMPUTATIONAL DETAILS

All the calculations in this research have been performed with the GAUSSIAN 03 suite of programs.[35] The geometries of all compounds were fully optimized and verified with subsequent vibrational analysis to be minima on their respective potential energy surface. Density functional theory in the form of Becke's[36] three-parameter hybrid functional (B3) with the nonlocal correlation of Lee−Yang−Parr (LYP)[37] has been employed together with the 6-311+G* basis set. Previously, this level of theory has been successfully used to study six member inorganic heterocycles $[BAlGaNPAs]_6$ and their dimers.[33] As shown for $[HAlYH]_n$ oligomers (Y = N, P; n = 1−4) results from B3LYP functional give quite satisfactory agreement with those obtained at CCSD(T)/cc-PVTZ level.[23,38] Accordingly, in the present work this level of theory has been applied to study structural, electronic, and thermodynamic properties of mixed heptamer clusters as well as $[(HM)_7(YH)_7]$ parents. A comparison of geometric parameters for the experimentally known heptamers and those calculated at the B3LYP/6-311+G* level (Supporting Information, Table S1) reveals that this level of theory can produce reliable results for group 13−15 heptamers.

3. RESULTS AND DISCUSSION

Previous investigations have shown that the potential energy surfaces of heteroatomic clusters are rich of stable local minima very close in energy. In such kind of potential energy surfaces, the determination of the ground state is not an easy task. Although the scope of this paper is not characterization of all possible isomers, the identification of the correct ground state is important because there is a strong dependence between various properties and cluster shape. Timoshkin et al.[16,39] in their extensive studies on group 13−15 oligomers have demonstrated that for $[(HM)_n(YH)_n]$ with high oligomerization degrees n = 7−16, the needle-shaped oligomers are more stable than the cage (fullerene-like) isomers. Herein, relying on the previous investigation, we considered the needle-shaped structure for all studied species. Two series of compounds were investigated; in series **I** the metal center of group 13 elements varies with preserving the nitrogen atom (compounds of the general formula $[(HM)_k(HM')_l(NH)_7]$; M,M′ = B, Al, Ga and $k + l = 7$) and in series **II** nonmetal centers change with the fixed group 13 element which is considered gallium (general formula of the species is $[(HGa)_7(YH)_m(Y'H)_n]$; Y,Y′ = N, P, As and $m + n = 7$).

Three stochiometric ratios are possible for the heptamers of each series. M:M′ ratio can be 6:1, 5:2, and 4:3 for the first series and similar Y:Y′ ratios can be considered for the mixed heptamers of series **II**. General structure of $[(HM)_7(YH)_7]$ cluster shown in Figure 1a indicates that a needle-shaped

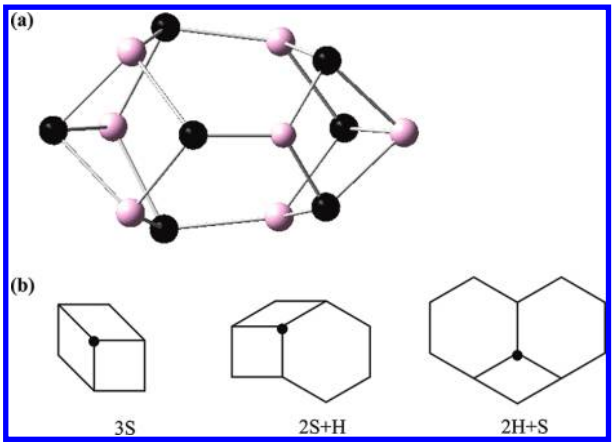

Figure 1. (a) General structure of needle-shaped binary heptamer cluster $[(HM)_7(YH)_7]$. Black and pink spheres are atoms of group 13 (M = B, Al, Ga) and group 15 (Y = N, P, As) (Hydrogen atoms are not shown). (b) Schematic view of 3S, 2S+H, and 2H+S positions in mixed ternary heptamers.

heptamer consists of nine faces including three hexagonals and six squares. Following the notation used in the work of Zurek et al.[40] and Timoshkin and Schaefer,[39] we classify isomers by the number of atoms in particular positions. 3S refers the structure in which the exchanged atom (M′ or Y′) shares three square faces, 2S+H describes sharing between two square faces and one hexagonal face, while 2H+S indicates that the impurity shares two hexagonal faces and one square face (Figure 1b). Accordingly, the number of possible isomers for ratios 6:1, 5:2, and 4:3 are, respectively, 3, 6, and 10. Considering the stochiometric ratios, the number of isomers in each ratio, and the metal or nonmetal (M′ or Y′) variation, we found 114 mixed heptamers in each series.

All 228 structures (Supporting Information, Tables S2 and S3) were fully optimized at the B3LYP/6-311+G* level of theory, and all optimized geometries were confirmed as minima by harmonic vibrational frequency calculation. Tables 1 and 2 list the lowest-energy isomer for each composition ratio in series **I** and **II**. It is obvious that the structure of the most stable isomer is dependent on its composition. For instance, consider the M:M′ stochiometric ratio to be 6:1, the position of the impurity atom in the lowest-energy isomer is 3S for M = Al and M′ = B, Ga while it is 2H+S for M = Ga, M′ = B and Al. From Table 2 we see that in series **II**, when Y:Y′ is 6:1, the position of impurity atom is 2H+S for Y = N and Y′ = P, As while it is 3S for Y = P, Y′ = N and As. Similarly, the positions of inserted atoms (M′ or Y′) are not fixed in the lowest-energy isomers for the other two composition ratios.

To facilitate our analysis, among all 228 optimized mixed heptamers, we just focus on the structural analysis and thermodynamic characteristics of the 36 lowest-energy structures reported in Tables 1 and 2.

dx.doi.org/10.1021/jp302323x | J. Phys. Chem. A 2012, 116, 4678−4686

3.1. Structural Analysis. An analysis of structural deviations between the calculated bond lengths or bond angles for the heteronuclear mixed heptamers and their corresponding homonuclear parents gives insight into the influence of the nature of group 13 and group 15 elements on the structure of mixed heptamers. Accordingly, important geometrical parameters of the 36 lowest-energy structures of mixed heptamers under investigation are listed in Tables 3 and 4 for series **I** and **II**, respectively. For the sake of comparison the geometrical parameters of parent homonuclear species have also been included. The results in Table 3 reveal that in most cases M′-insertion in $[(HM)_7(NH)_7]$ generates ternary composites in which M−N bonds are longer than M−N bonds in binary homonuclear $[(HM)_7(NH)_7]$ species. The changes in M−N bond lengths because of M′-insertion are considered as $\%\Delta R = (R - R_o) \times 100$, where R is the average of M−N bond lengths in the mixed heptamer and R_o corresponds to the average of M−N bond lengths in the binary homonuclear parent. The computed $\%\Delta R$ for B−N bond lengths reveal that the maximum elongation (0.39%) has occurred in $[(HB)_5(HAl)_2(NH)_7]$, while for the rest of the $[(HB)_k(HM')_l[(NH)_7]$ species with M′ = Al and Ga, $\%\Delta R$ ranges from 0.05% to 0.24%. The calculated increments in the Ga−N bond as a result of Al-insertion in $[(HGa)_7(NH)_7]$ are much larger than computed $\%\Delta R$ for B- insertion. In contrast to B−N and Ga−N bonds, the Al−N bonds in $[(HAl)_7(NH)_7]$ are contracted by about 0.07% to 0.86% when Al is exchanged by either B or Ga.

For the studied compounds in series **II** in most cases exchanging Y atoms by Y′ in $[(HGa)_7(YH)_7]$ generates ternary composites in which Ga−Y bonds are shorter than Ga−Y bonds in binary homonuclear $[(HGa)_7(YH)_7]$ species (see Table 4). For Ga−As and Ga−P bonds the contractions range from −0.09% to −0.71% and −0.04% to −0.59%, respectively. On the contrary, in the case of Ga−N, the bond length elongation in the range between 0.45% and 1.10% has been observed. In general, inserting M′ or Y′ into a binary $[(HM)_7(YH)_7]$ clusters leads to some geometrical distortion which can be attributed to the difference between atomic radii and electronegativities of M and M′ or Y and Y′. However, the computed variations in geometrical parameters are small, and the structures of ternary composites found through optimization with no constraint retain the shape of their homonuclear parent heptamers.

3.2. Thermodynamic Characteristics. The thermodynamic properties for the formation of 36 lowest-energy structures of mixed heptamers from the corresponding group 13 and group 15 hydrides are provided in the Table 5 for the reactions 1 and 2,

$$\frac{k}{7}MH_3 + \frac{l}{7}M'H_3 + NH_3 \rightarrow \frac{1}{7}[(HM)_k(HM')_l(NH)_7] + 2H_2 \quad (1)$$

$$GaH_3 + \frac{m}{7}YH_3 + \frac{n}{7}Y'H_3 \rightarrow \frac{1}{7}[(HGa)_7(HY)_m(HY')_n] + 2H_2 \quad (2)$$

In series **I**, we found that insertion of aluminum atom in $[(HB)_7(NH)_7]$ binary oligomer is energetically favorable while entering gallium atoms disfavors the process of mixed cluster generation in this case. For instance, compare ΔH^0_{298} for the pairs $[(HB)_6(HAl)(NH)_7]$ and $[(HB)_6(HGa)(NH)_7]$. In general, formation of $[(HB)_k(HAl)_l(NH)_7]$ species are about 1.81 to 6.15 kcal mol^{-1} more favorable than $[(HB)_7(NH)_7]$, while $[(HB)_k(HGa)_l(NH)_7]$ oligomers are 1.79−4.60 kcal mol^{-1} less favored. This diversity can be attributed to electronegativity difference between metal and nonmetal centers. The electronegativity difference between Al and N is greater than in BN and GaN which results in stronger electrostatic attraction. Moreover, because of greater dissociation energy of Al−N compared to Ga−N bond, the aluminum containing compounds exhibit enhanced stability.

Considering the $[(HAl)_7(NH)_7]$ oligomer in series **I**, we found that replacing Al atoms by boron or gallium atoms is

Table 1. Total Electronic Energy and Zero Point Vibrational Energy (ZPE) for the Lowest-Energy Structures of Mixed Heptamers in Series I.[a]

M	M′	k	l	position of exchanged atom(s)	total energy	ZPE
B	Al	6	1	2S+H	−783.897695	135.96
B	Al	5	2	2S+H, 2S+H	−1001.52965	131.34
B	Al	4	3	2S+H, 2S+H, 2S+H	−1219.165937	126.69
B	Ga	6	1	2S+H	−2466.267882	135.49
B	Ga	5	2	2S+H, 2S+H	−4366.269866	130.29
B	Ga	4	3	2S+H, 2S+H, 2S+H	−6266.277113	125.25
Al	B	6	1	3S	−1872.071881	112.34
Al	B	5	2	3S, 2H+S	−1654.432748	117.14
Al	B	4	3	2H+S, 2H+S, 3S	−1436.797088	121.91
Al	Ga	6	1	3S	−3772.07833	107.68
Al	Ga	5	2	3S, 2S+H	−5454.448555	107.22
Al	Ga	4	3	2S+H, 2S+H, 3S	−7136.818162	106.65
Ga	B	6	1	2H+S	−11966.27821	109.73
Ga	B	5	2	3S, 2H+S	−10066.27669	114.57
Ga	B	4	3	2H+S, 2H+S, 3S	−8166.274803	119.83
Ga	Al	6	1	2H+S	−12183.92115	105.08
Ga	Al	5	2	2H+S, 2H+S	−10501.55452	105.66
Ga	Al	4	3	2H+S, 2H+S, 2H+S	−8819.187472	106.16

[a]Total electronic energies are in Hartree and ZPE values are in kcal mol^{-1}.

dx.doi.org/10.1021/jp302323x | J. Phys. Chem. A 2012, 116, 4678−4686

Table 2. Total Electronic Energy and Zero Point Vibrational Energy (ZPE) for the Lowest-Energy Structures of Mixed Heptamers in Series II.[a]

Y	Y′	*m*	*n*	position of exchanged atom(s)	total energy	ZPE
N	P	6	1	2H+S	−14152.87158	100.56
N	P	5	2	2H+S, 2H+S	−14439.4601	96.56
N	P	4	3	2H+S, 2H+S, 2H+S	−14726.05258	92.72
N	As	6	1	2H+S	−16047.37579	99.56
N	As	5	2	2H+S, 2H+S	−18228.47023	94.42
N	As	4	3	2H+S, 2H+S, 2H+S	−20409.56954	89.69
P	N	6	1	3S	−15585.83398	81.04
P	N	5	2	2H+S,3S	−15299.23631	84.88
P	N	4	3	2S+H, 2S+H, 2S+H	−15012.64704	88.91
P	As	6	1	3S	−17766.93602	76.29
P	As	5	2	2H+S, 3S	−19661.44315	75.37
P	As	4	3	2H+S, 2H+S, 3S	−21555.95033	74.38
As	N	6	1	3S	−26952.87358	74.97
As	N	5	2	2H+S, 3S	−24771.76799	79.93
As	N	4	3	2S+H, 2S+H, 2S+H	−22590.67381	84.99
As	P	6	1	2S+H	−27239.47123	71.50
As	P	5	2	2S+H, 2S+H	−25344.96434	72.60
As	P	4	3	2S+H, 2S+H, 2S+H	−23450.45757	73.25

[a]Total electronic energies are in hartree and ZPE values are in kcal mol^{-1}.

Table 3. Calculated Bond Lengths (Å) and Bond Angles (deg) for the Lowest-Energy Structures of Mixed Heptamers in Series I

M	M′	*k*	*l*	M−N	M′−N	N−M−N	M−N−M
B	Al	6	1	1.587	1.925	92.2, 105.6, 113.6	86.5, 115.2, 121.2
B	Al	5	2	1.589	1.931	94.6, 113.9	91.2, 115.0, 121.0
B	Al	4	3	1.586	1.941	92.0, 115.2	86.3, 120.1
B	Ga	6	1	1.586	1.994	92.1, 102.2, 112.7	87.1, 118.5
B	Ga	5	2	1.586	1.995	91.9, 102.1, 114.0	86.6, 120.2
B	Ga	4	3	1.584	1.999	92.0, 115.6	86.2, 120.7
Al	B	6	1	1.932	1.611	85.2, 109.9	89.8, 122.4
Al	B	5	2	1.933	1.597	87.4, 104.1, 110.4	89.8, 114.9, 125.3
Al	B	4	3	1.936	1.591	79.4, 91.4, 106.7	89.84, 117.3
Al	Ga	6	1	1.935	2.010	89.7, 108.7	89.7, 121.1
Al	Ga	5	2	1.931	2.011	90.0, 109.7	89.9, 121.1
Al	Ga	4	3	1.928	2.009	90.2, 110.1	120.4
Ga	B	6	1	1.994	1.595	87.3, 106.5	91.2, 114.1, 125.2
Ga	B	5	2	1.992	1.592	88.2, 104.9, 113.3	91.6, 113.8
Ga	B	4	3	1.995	1.588	88.2, 105.4	91.5, 116.7
Ga	Al	6	1	1.997	1.922	87.5, 106.4	91.1, 121.0
Ga	Al	5	2	2.001	1.923	87.4, 103.5, 110.3	90.9, 121.6
Ga	Al	4	3	2.005	1.925	86.8, 103.3	91.3
binary parents							
$[(HB)_7(NH)_7]$				1.585		92.3, 111.0	86.5, 115.4, 121.0
$[(HAl)_7(NH)_7]$				1.937		89.1, 104.2, 111.5	89.8, 120.6
$[(HGa)_7(NH)_7]$				1.994		87.5, 103.9, 111.0	91.2, 121.2

Table 4. Calculated Bond Lengths (Å) and Bond Angles (deg) for the Lowest-Energy Structures of Mixed Heptamers in Series II

Y	Y′	*m*	*n*	Y−Ga	Y′−Ga	Ga−Y−Ga	Y−Ga−Y
N	P	6	1	1.999	2.401	91.1, 100.2, 122.3	87.3, 107.2, 116.9
N	P	5	2	2.002	2.410	91.0, 101.0, 124.0	87.0, 115.7
N	P	4	3	2.004	2.416	97.1, 101.0, 124.2	86.4
N	As	6	1	1.999	2.488	91.4, 102.0, 123.2	87.0, 109.5, 118.0
N	As	5	2	2.003	2.501	90.9, 124.5	86.9, 116.4
N	As	4	3	2.005	2.506	90.2, 102.8, 125.2	86.4
P	N	6	1	2.425	2.015	89.2, 121.9	86.6, 105.7, 111.5
P	N	5	2	2.425	2.007	89.8, 118.1, 128.6	86.4, 108.7
P	N	4	3	2.428	2.001	90.5, 120.6	90.9
P	As	6	1	2.429	2.536	91.8, 102.6, 121.0	86.6, 102.6, 111.0
P	As	5	2	2.431	2.528	92.0, 120.5	86.8, 103.3, 111.7
P	As	4	3	2.430	2.526	91.3, 120.6	86.7, 112.0
As	N	6	1	2.520	2.018	86.0, 119.5, 125.7	86.2, 105.7, 111.1
As	N	5	2	2.520	2.009	77.9, 91.7, 118.3	88.5, 111.2
As	N	4	3	2.523	2.001	90.8, 120.0	89.1, 98.0
As	P	6	1	2.526	2.438	90.8, 120.8	87.7, 102.4, 110.8
As	P	5	2	2.525	2.435	90.6, 121.6	98.2, 110.7
As	P	4	3	2.525	2.433	91.2, 122.5	88.6, 101.6
binary parents							
$[(HGa)_7(NH)_7]$				1.994		91.2, 121.1	87.5, 103.9, 111.0
$[(HGa)_7(PH)_7]$				2.431		90.9, 121.0	87.9, 102.9, 111.0
$[(HGa)_7(AsH)_7]$				2.527		91.1, 120.9	87.4, 102.6, 110.9

energetically disfavored. For example, the enthalpy of formation shows that $[(HAl)_6(HB)(NH)_7]$ and $[(HAl)_6(HGa)(NH)_7]$ are, respectively 2.30 and 3.59 kcal mol^{-1} less stable than $[(HAl)_7(NH)_7]$. Finally, inserting boron or aluminum atoms in the $[(HGa)_7(NH)_7]$ heptamer, energetically stabilizes the

dx.doi.org/10.1021/jp302323x | J. Phys. Chem. A 2012, 116, 4678−4686

Table 5. Thermodynamic Characteristics for the Formation of Mixed Heptamers in Series I and II According to Reactions 1 and 2[a]

		$[(HM)_k(HM')_l(HN)_7]$				$[(HGa)_7(YH)_m(Y'H)_n]$					
M	M′	k	l	ΔH^0_{298}	ΔS^0_{298}	Y	Y′	m	n	ΔH^0_{298}	ΔS^0_{298}
B		7	0	−41.84	−21.63	N		7	0	−30.92	−20.22
B	Al	6	1	−43.65	−21.66	N	P	6	1	−29.59	−19.69
B	Al	5	2	−45.63	−21.68	N	P	5	2	−28.70	−19.16
B	Al	4	3	−47.99	−21.72	N	P	4	3	−28.15	−18.64
B	Ga	6	1	−40.05	−21.47	N	As	6	1	−29.63	−19.97
B	Ga	5	2	−38.42	−21.27	N	As	5	2	−28.95	−19.66
B	Ga	4	3	−37.24	−21.10	N	As	4	3	−28.65	−19.42
Al		7	0	−57.17	−21.78	P		7	0	−26.51	−16.72
Al	B	6	1	−54.87	−21.62	P	N	6	1	−26.85	−17.19
Al	B	5	2	−52.24	−21.65	P	N	5	2	−26.94	−17.69
Al	B	4	3	−49.91	−21.67	P	N	4	3	−27.76	−18.16
Al	Ga	6	1	−53.58	−21.53	P	As	6	1	−26.80	−16.98
Al	Ga	5	2	−49.97	−21.33	P	As	5	2	−27.09	−17.27
Al	Ga	4	3	−46.32	−21.10	P	As	4	3	−27.40	−17.54
Ga		7	0	−30.92	−20.22	As		7	0	−28.52	−18.68
Ga	B	6	1	−31.88	−20.48	As	N	6	1	−28.38	−18.78
Ga	B	5	2	−33.59	−20.57	As	N	5	2	−28.08	−19.06
Ga	B	4	3	−35.24	−20.83	As	N	4	3	−28.80	−19.29
Ga	Al	6	1	−34.83	−20.45	As	P	6	1	−28.24	−18.39
Ga	Al	5	2	−38.75	−20.67	As	P	5	2	−27.95	−18.14
Ga	Al	4	3	−42.64	−20.89	As	P	4	3	−27.72	−17.79

[a]Standard enthalpies, ΔH^0_{298}, are in kcal mol^{-1} and standard entropies, ΔS^0_{298}, are given in cal mol^{-1} K^{-1}.

formation of ternary clusters. The numerical results in Table 5 show that the exothermicity of reaction 1 increases as the number of Al−N and B−N bonds increase.

Now turning our attention to reaction 2, at first glance it is observed that the variations of thermodynamic properties are less pronounced in second series of studied heptamers when the nonmetal center varies. In general, considering $[(HGa)_7(YH)_7]$ as parent heptamer we see that inserting the second nonmetal element of group 15, Y′, irrespectively of its nature disfavors the generation of mixed heptamer. This may be due to structural deviation caused by steric effects associated with nonmetal elements with different sizes. The only exception is $[(HGa)_7(PH)_7]$ species, in which replacement of each phosphorus by either nitrogen or arsenic leads to little stabilization (less than 1 kcal mol^{-1}) through the formation of mixed cluster.

In another view we compare the stability of the mixed clusters with respect to the constituent mixture of monomers in reactions 3 and 4.

$$k[(HM)(NH)] + l[(HM')(NH)] \rightarrow [(HM)_k(HM')_l(NH)_7] \quad (3)$$

$$m[(HGa)(YH)] + n[(HGa)(Y'H)] \rightarrow [(HGa)_7(YH)_m(Y'H)_n] \quad (4)$$

The thermodynamic properties for the given processes in reactions 3 and 4 are collected in Table 6. The results indicate that in the first series, the favorability of the cluster formation increases as the number of Al atoms in the heptamer increases which can be attributed to the substantially higher group 13−15 bond energy in such species.[41] Similarly, in series **II** heptamers containing more nitrogen atoms are more stable.

In general, as can be seen from the data reported in Tables 5 and 6, generation of mixed heptamers through corresponding group 13 and group 15 hydrides or monomers is strongly exothermic and thermodynamically favorable. The entropy factor disfavors the process of cluster generation; however, this effect is not strong enough to prevent formation of mixed heptamers in the gas phase.

Finally, it is also of interest to compare the stability of the mixed clusters with respect to the mixture of homonuclear heptamers having the same composition (reactions 5 and 6).

$$[(HM)_k(HM')_l(NH)_7] \rightarrow \frac{k}{7}[(HM)_7(NH)_7] + \frac{l}{7}[(HM')_7(NH)_7] \quad (5)$$

$$[(HGa)_7(YH)_m(Y'H)_n] \rightarrow \frac{m}{7}[(HGa)_7(YH)_7] + \frac{n}{7}[(HGa)_7(Y'H)_7] \quad (6)$$

It is found that in series **I** with a single exception in $[(HAl)_k(HGa)_l(NH)_7]$ compounds, the processes of the reorganization of the mixed ternary clusters into mixture of binary heptamers are favored by enthalpy while the entropy changes are not significant (see Supporting Information, Table S4). For the$[(HM)_k(HM')_l(NH)_7]$ compounds, values lie in range −1.57 to −4.78 kcal mol^{-1} for the enthalpy, and less than 0.3 cal mol^{-1} K^{-1} for the entropy of the reaction 5. For the species in series **II**, the process of their reorganization into homonuclear binary heptamers is much more favorable for the nitrogen-containing compounds (enthalpies of the reaction 6 lie in range between −2.03 to −8.98 kcal mol^{-1} while the changes in entropy are slightly disfavored. For the P and As containing heptamers both ΔH^0_{298} and ΔS^0_{298} values of reaction 6 are near to zero. Because of higher exothermicity of the

dx.doi.org/10.1021/jp302323x | J. Phys. Chem. A 2012, 116, 4678−4686

Table 6. Thermodynamic Characteristics for the Formation of Mixed Heptamers in Series I and II According to Reactions 3 and 4[a]

		$[(HM)_k(HM')_l(HN)_7]$				$[(HGa)_7(YH)_m(Y'H)_n]$					
M	M′	k	l	ΔH^0_{298}	ΔS^0_{298}	Y	Y′	m	n	ΔH^0_{298}	ΔS^0_{298}
B		7	0	−271.01	−205.80	N		7	0	−521.71	−399.37
B	Al	6	1	−328.00	−216.88	N	P	6	1	−488.08	−278.32
B	Al	5	2	−386.06	−227.87	N	P	5	2	−457.45	−277.28
B	Al	4	3	−446.88	−238.98	N	P	4	3	−429.18	−276.36
B	Ga	6	1	−305.25	−216.54	N	As	6	1	−480.59	−278.19
B	Ga	5	2	−340.54	−227.06	N	As	5	2	−443.68	−276.73
B	Ga	4	3	−328.00	−237.83	N	As	4	3	−409.48	−275.75
Al		7	0	−688.09	−282.87	P		7	0	−320.25	−427.19
Al	B	6	1	−627.78	−270.88	P	N	6	1	−347.01	−274.35
Al	B	5	2	−565.07	−260.24	P	N	5	2	−372.00	−275.18
Al	B	4	3	−504.56	−249.52	P	N	4	3	−402.13	−275.68
Al	Ga	6	1	−665.47	−282.22	P	As	6	1	−314.54	−273.62
Al	Ga	5	2	−642.69	−281.79	P	As	5	2	−308.83	−273.60
Al	Ga	4	3	−619.63	−281.26	P	As	4	3	−303.21	−273.47
Ga		7	0	−521.71	−399.37	As		7	0	−280.05	−446.46
Ga	B	6	1	−481.70	−269.14	As	N	6	1	−311.19	−273.29
Ga	B	5	2	−446.98	−257.88	As	N	5	2	−341.25	−274.56
Ga	B	4	3	−411.74	−247.81	As	N	4	3	−378.41	−275.47
Ga	Al	6	1	−546.65	−279.84	As	P	6	1	−285.87	−273.32
Ga	Al	5	2	−571.58	−280.36	As	P	5	2	−291.59	−273.61
Ga	Al	4	3	−596.32	−280.79	As	P	4	3	−297.73	−273.16

[a]Standard enthalpies, ΔH^0_{298}, are in kcal mol^{-1} and standard entropies, ΔS^0_{298}, are given in cal mol^{-1} K^{-1}.

Table 7. Calculated Band Gap and Electric Dipole Moments for Mixed Heptamers in Series I and II[a]

		$[(HM)_k(HM')_l(HN)_7]$				$[(HGa)_7(YH)_m(Y'H)_n]$					
M	M′	k	l	gap	μ	Y	Y′	m	n	gap	μ
B		7	0	6.95	1.45	N		7	0	6.67	1.54
B	Al	6	1	6.82	1.50	N	P	6	1	6.17	1.15
B	Al	5	2	6.78	1.49	N	P	5	2	5.79	0.73
B	Al	4	3	6.85	1.48	N	P	4	3	5.56	0.36
B	Ga	6	1	6.54	1.91	N	As	6	1	5.99	1.07
B	Ga	5	2	6.44	2.06	N	As	5	2	5.43	0.55
B	Ga	4	3	6.49	2.12	N	As	4	3	5.08	0.02
Al		7	0	7.02	2.05	P		7	0	5.12	0.87
Al	B	6	1	7.03	2.06	P	N	6	1	5.09	1.10
Al	B	5	2	6.89	1.75	P	N	5	2	5.12	1.51
Al	B	4	3	6.87	1.62	P	N	4	3	5.27	0.03
Al	Ga	6	1	6.99	1.08	P	As	6	1	5.01	0.63
Al	Ga	5	2	6.83	1.58	P	As	5	2	4.91	0.56
Al	Ga	4	3	6.74	1.86	P	As	4	3	4.87	0.50
Ga		7	0	6.67	1.54	As		7	0	4.72	0.66
Ga	B	6	1	6.38	1.28	As	N	6	1	4.62	1.02
Ga	B	5	2	6.47	2.23	As	N	5	2	4.69	1.52
Ga	B	4	3	6.42	2.18	As	N	4	3	4.98	0.44
Ga	Al	6	1	6.62	1.85	As	P	6	1	4.74	0.64
Ga	Al	5	2	6.61	2.01	As	P	5	2	4.79	0.55
Ga	Al	4	3	6.66	2.01	As	P	4	3	4.87	0.44

[a]Band gaps are given in eV and dipole moments are in Debye.

reorganization process in case of $[(HGa)_7(YH)_m(Y'H)_n]$ species, the temperatures that favor mixed species in series **II** are higher than what is estimated for heptamers of series **I**.

3.3. Band Gap and Dipole Moment Analysis. Another important characteristic of group 13−15 clusters is the gap between the highest occupied molecular orbital (HOMO) and the lowest unoccupied molecular orbital (LUMO). The numerical values of calculated band gaps of the 36 lowest-energy structures of the mixed heptamers are listed in Table 7, and their variations with respect to exchanged atoms are shown in Figures 2 and 3 for series **I** and **II**, respectively. To have a meaningful comparison, these tables and figures include the band gaps of the parent homonuclear heptamers, too.

dx.doi.org/10.1021/jp302323x | J. Phys. Chem. A 2012, 116, 4678−4686

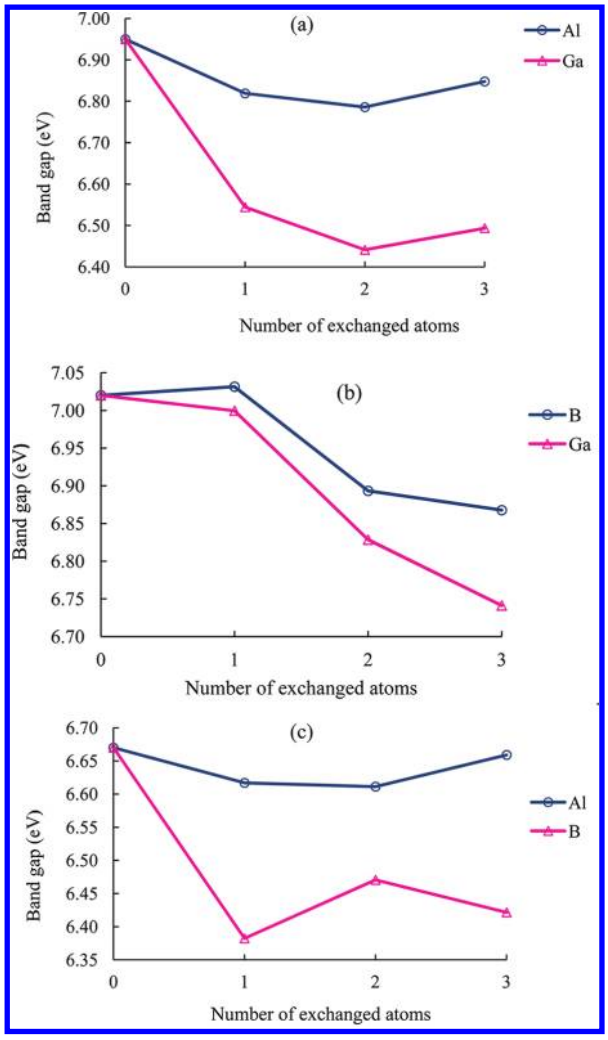

Figure 2. Trends in the band gap of heptamers of series **I**. (a) parent is $[(HB)_7(NH)_7]$ and M′ = Al, Ga, (b) parent is $[(HAl)_7(NH)_7]$ and M′ = B, Ga, (c) parent is $[(HGa)_7(NH)_7]$ and M′ = Al, B.

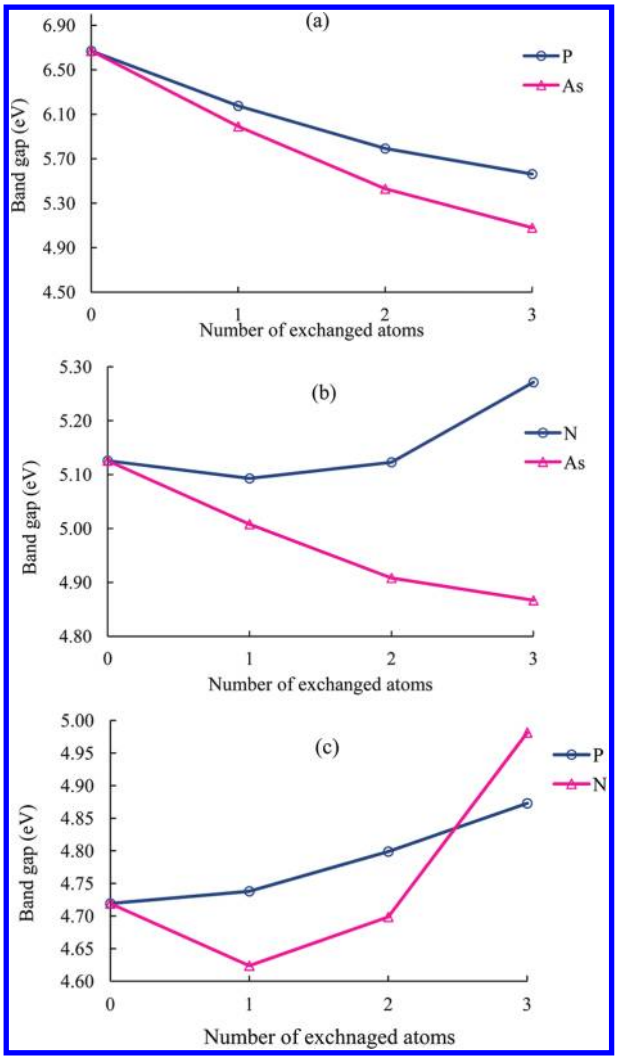

Figure 3. Trends in band gap of heptamers of series **II**. (a) Parent is $[(HGa)_7(NH)_7]$ and Y′ = P, As, (b) parent is $[(HGa)_7(PH)_7]$ and Y′ = N, As, (c) parent is $[(HGa)_7(AsH)_7]$ and Y′ = P, N.

Commencing with the $[(HB)_7(NH)_7]$ cluster in series **I**, the first observation is the reduction of band gap because of exchanging boron atoms by Al or Ga; however, the reduction is more sensible for gallium insertion (Figure 2a). For the inclusion of boron in $[(HAl)_7(NH)_7]$ (gap = 7.02 eV), after a small enhancement in $[(HAl)_6(HB)(NH)_7]$ (gap = 7.03 eV) the band gap reduces to 6.87 eV in $[(HAl)_4(HB)_3(NH)_7]$ (Figure 2b). Moreover, Figure 2b shows that Ga insertion accompanies with decrease in band gap of $[(HAl)_7(NH)_7]$ by about 0.03, 0.19, and 0.28 eV for $[(HAl)_6(HGa)(NH)_7]$, $[(HAl)_5(HGa)_2(NH)_7]$ and $[(HAl)_4(HGa)_3(NH)_7]$, respectively. Comparison of $[(HGa)_6(HB)(NH)_7]$ and $[(HGa)_7(NH)_7]$ in Figure 2c indicates a significant band gap reduction (0.29 eV) because of insertion of boron while inclusion of the second boron in $[(HGa)_5(HB)_2(NH)_7]$ increases the band gap by about 0.09 eV with respect to $[(HGa)_6(HB)(NH)_7]$. On the contrary, Al-insertion has no significant effect on the band gap of $[(HGa)_7(NH)_7]$ cluster.

In series **II**, in the $[(HGa)_7(NH)_7]$ family (Figure 3a) inclusion of both phosphorus and arsenic leads to similar behavior of band gap reduction. Starting from $[(HGa)_7(PH)_7]$ in the second group and replacing one phosphorus by either N or As reduces the band gap while different trends have been observed for the insertion of two or three N or As. Figure 3b shows that inclusions of second and the third nitrogens increase the band gap by about 0.03 and 0.16 eV with respect to the $[(HGa)_7(NH)(PH)_6]$ species. On the other hand, insertion of second and third arsenics leads to a 0.10 and 0.14 eV decrease in the band gap with respect to $[(HGa)_7(AsH)(PH)_6]$. Finally, in the last group of $[(HGa)_7(AsH)_7]$ (gap = 4.72 eV) it is observed that insertion of phosphorus leads to a smooth increase in the calculated band gap. In the case of nitrogen insertion, after a reduction of the band gap in $[(HGa)_7(PH)(AsH)_6]$ (gap = 4.62 eV), the band gaps climb to 4.69 and 4.98 eV in $[(HGa)_7(NH)_2(AsH)_5]$ and $[(HGa)_7(NH)_3(AsH)_4]$, respectively.

An overall inspection of the calculated band gaps for the 36 lowest-energy structures of the studied mixed heptamers concludes that the band gaps of ternary compounds of series **II** lie in lower range in comparison to the first series compounds. Among all studied heptamers, the smaller band gaps correspond to the arsenic containing heptamers which lie close to the semiconducting regime, around 4.62−4.98 eV.

It is also noteworthy to mention that a particularly difference between series **I** and series **II** is the extent of charge separation in the studied heptamers. The calculated dipole moments for the 36 lowest-energy structures of mixed heptamers as well as

dx.doi.org/10.1021/jp302323x | J. Phys. Chem. A 2012, 116, 4678−4686

their corresponding binary parents are also provided in Table 7. In general, the electric dipole moments of the compounds in series **I** are substantially greater than those of the studied heptamers of series **II**. We found that variation of electric dipole moment correlates with the localization or delocalization pattern of the frontier orbitals. Delocalization of the HOMO and LUMO orbitals results in a smaller band gap which in turn leads to easier charge transfer and smaller dipole moment. Comparing the calculated electric dipole moment with the orbital pictures confirms that heptamers of series **I** with more localized frontier orbitals and consequently greater band gaps have greater dipole moments. Moreover, the smallest dipole moments of the arsenic containing family heptamers are consistent with their smaller band gap value which has been mentioned before.

4. CONCLUSIONS

We have investigated the structural characteristics, thermodynamic and electronic properties of group 13−15 needle-shaped mixed heptamers in two series; series **I** with general formula $[(HM)_k(HM')_l(HN)_7]$ (M, M′ = B, Al, Ga and $k + l = 7$) and series **II** with general formula $[(HGa)_7(YH)_m(Y'H)_n]$ (Y,Y′ = N, P, As and $m + n = 7$). From the structural point of view we found that mixed heptamers retain the shape of their homonuclear parent clusters, that is, $[(HM)_7(HN)_7]$ and $[(HGa)_7(YH)_7]$ for seires **I** and **II**, respectively. However, bond lengths and bond angles undergo small variations through the insertion of M′ or Y′. In general, we found that the variations in bond lengths and bond angles are less sensible in the second series of studied heptamers comparing to series **I**.

On the other hand, analysis of thermodynamic properties reveals that all 36 lowest-energy structures of the studied mixed heptamer species are stable as their homonuclear analogues. We considered two aspects for the formation of mixed heptamers: cluster formation from the corresponding group 13 and group 15 hydrides and oligomerization reactions from monomers. It is indicated that the favorability for the generation of mixed heptamers strongly depends on the nature of inserted metal and nonmetal pairs of group 13−15. Among all studied heptamers aluminum-containing clusters show the higher stability which is due to the substantially higher group 13−15 bond energy in such species.

An overall inspection of the calculated band gaps for all 36 studied mixed heptamers concludes that the band gaps of ternary compounds of series **II** lie in the lower range in comparison to those of the first series compounds. We found that the smallest band gaps correspond to arsenic containing heptamers which lie close to the semiconducting regime, around 4.62−4.98 eV. Moreover, analysis of dipole moments indicates that polarity of mixed heptamers correlates with their band gaps. Delocalization of frontier orbitals results in a smaller band gap which in turn leads to easier charge transfer and smaller dipole moment.

■ ASSOCIATED CONTENT

Supporting Information

Table S1 presents a comparison of geometric parameters for the experimentally known heptamers and those calculated at the B3LYP/6-311+G* level. Tables S2 and S3 list all 228 studied species as well as the position of the exchanged atoms and relative energies of different isomers with respect to the lowest-energy isomer for each composition ratio. Table S4 collects thermodynamic characteristics for the formation of mixed heptamers in series **I** and **II** according to reactions 5 and 6. Moreover, the optimized geometries of the lowest-energy structures of studied mixed heptamers at B3LYP/6-311+G* level are also reported. This material is available free of charge via the Internet at http://pubs.acs.org.

■ AUTHOR INFORMATION

Corresponding Author

*Phone: +98 7116137520. Fax: +98 7112286008. E-mail: amohajeri@shirazu.ac.ir.

Notes

The authors declare no competing financial interest.

■ REFERENCES

(1) Trindade, T.; Óbrien, P.; Pickett, N. L. *Chem. Mater.* **2001**, *13*, 3843−3858.
(2) Aldridge, S., Downs, A. J., Eds.; *The Group 13 Metals Aluminium, Gallium, Indium and Thallium: Chemical Patterns and Peculiarities*; Wiley: Chichester, U.K., 2011.
(3) Atwood, D. A.; Cowley, A. H.; Jones, R. A.; Mardones, M. A. *J. Organomet. Chem.* **1993**, *449*, C1−C2.
(4) Cowley, A. H.; Jones, R. A. *Polyhedron* **1994**, *13*, 1149−1157.
(5) Jouet, R. J.; Purdy, A. P.; Wells, R. L.; Janik, J. F. *J. Cluster Sci.* **2002**, *13*, 469−486.
(6) Denis, J.-M.; Forintos, H.; Szelke, H.; Toupet, L.; Pham, T.-N.; Madec, P.-J.; Gaumont, A.-C. *Chem. Commun.* **2003**, 54−55.
(7) Marder, T. B. *Angew. Chem., Int. Ed.* **2007**, *46*, 8116−8118.
(8) Langmi, H. W.; McGrady, G. S. *Coord. Chem. Rev.* **2007**, *251*, 925−935.
(9) Clark, T. J.; Lee, K.; Manners, I. *Chem.—Eur. J.* **2006**, *12*, 8634−8648.
(10) Den Baars, S. P.; Keller, S. *Semicond. Semimet.* **1998**, *50*, 11−37.
(11) Stringfellow, G. B. *Organometallic Vapor-Phase Epitaxy: Theory and Practice*; Academic Press: New York, 1989.
(12) Timoshkin, A. Y. *Coord. Chem. Rev.* **2005**, *249*, 2094−2131.
(13) Hardman, N. J.; Cui, C.; Roesky, H. W.; Fink, W. H.; Power, P. P. *Angew. Chem., Int. Ed.* **2001**, *40*, 2172−2174.
(14) Wright, R. J.; Phillips, A. D.; Allen, T. L.; Fink, W. H.; Power, P. P. *J. Am. Chem. Soc.* **2003**, *125*, 1694−1695.
(15) Timoshkin, A. Y. *Russ. J. Phys. Chem. A* **2007**, *81*, 516−525. Demchuk, A.; Simpson, S.; Koplitz, B. *Electrochem. Soc. Proc.* **2001**, *13*, 389−396.
(16) Timoshkin, A. Y.; Schaefer, H. F. *J. Am. Chem. Soc.* **2004**, *126*, 12141−12154.
(17) Sauls, F. C.; Interrante, L. V. *Coord. Chem. Rev.* **1993**, *128*, 193−207.
(18) Carmalt., C. J. *Coord. Chem. Rev.* **2001**, *223*, 217−264.
(19) Timoshkin, A. Y. *Inorg. Chem. Commun.* **2003**, *6*, 274−277.
(20) Schaumlöffel, A.; Linnolahti, M.; Karttunen, A. J.; Pakkanen, T. A. *Chem. Phys. Chem.* **2007**, *8*, 62−63.
(21) Koromos, B. L.; Cramer, C. J.; Gladfelter, W. L. *J. Phys. Chem. A* **2006**, *110*, 494−502.
(22) Tanskanen, J. T.; Linnolahti, M.; Karttunen, A. J.; Pakkanen, T. A. *J. Phys. Chem. C* **2009**, *113*, 10065−10069.
(23) Timoshkin, A. Y.; Schaefer, H. F. *J. Phys. Chem. A* **2010**, *114*, 516−525.
(24) Mallajosyula, S. S.; Datta, A.; Pati, S. K. *J. Phys. Chem. A* **2006**, *110*, 5156−5163.
(25) Koromos, B. L.; Jegier, J. A.; Ewbank, P. C.; Permisz, U.; Young, V. G., Jr.; Cramer, C. J.; Gladfelter, W. L. *J. Am. Chem. Soc.* **2005**, *127*, 1493−1503.
(26) Tanskanen, J. T.; Linnolahti, M.; Karttunen, A. J.; Pakkanen, T. A. *J. Phys. Chem. C* **2009**, *113*, 229−234.
(27) Lisovenko, A. S.; Timoshkin, A. Y. *Inorg. Chem.* **2010**, *49*, 10357−10369.
(28) Timoshkin, A. Y.; Schaefer, H. F. *J. Phys. Chem. C* **2008**, *112*, 13816−13836.
(29) Nakamura, S. *Semicond. Semimet.* **1998**, *48*, 391−426.

(30) Ni, H.; York, D. M.; Bartolotti, L.; Wells, R. L.; Yang, W. *J. Am. Chem. Soc.* **1996**, *118*, 5732−5736.
(31) Foos, E. E.; Jouet, R. J.; Wells, R. L.; Rheingold, A. L.; Liable-Sands, L. M. *J. Organomet. Chem.* **1999**, *582*, 45−52.
(32) Jouet, R. J.; Wells, R. L.; Rheingold, A. L.; Incarvito, C. D. *J. Organomet. Chem.* **2000**, *601*, 191−198.
(33) Timoshkin, A. Y.; Frenking, G. *Inorg. Chem.* **2003**, *42*, 60−69.
(34) Timoshkin, A. Y. *Solid-State Electron.* **2003**, *47*, 543−548.
(35) Frisch, M. J.; Trucks, G. W.; Schlegel, H. B.; Scuseria, G. E.; Robb, M. A.; Cheeseman, J. R.; Montgomery, J. A., Jr.; Vreven, T.; Kudin, K. N.; Burant, J. C.; et al. *Gaussian 03*, Revision E.01; Gaussian Inc.: Wallingford, CT, 2004.
(36) Becke, A. D. *J. Chem. Phys.* **1993**, *98*, 5648−5652.
(37) Lee, C. L.; Yang, W.; Parr, R. G. *Phys. Rev. B* **1988**, *37*, 785−789.
(38) Timoshkin, A. Y.; Schaefer, H. F. *Inorg. Chem.* **2004**, *43*, 3080−3089.
(39) Timoshkin, A. Y.; Schaefer, H. F. *Inorg. Chem.* **2005**, *44*, 843−845.
(40) Zurek, E.; Woo, T. K.; Firman, T. K.; Ziegler, T. *Inorg. Chem.* **2001**, *40*, 361−370.
(41) Timoshkin, A. Y.; Bettinger, H. F.; Schaefer, H. F. *Inorg. Chem.* **2002**, *41*, 738−747.